Wide-Area Composite Load Parameter Identification Based on Multi-Residual Deep Neural Network

Shahabodin Afrasiabi, *Graduate Student Member, IEEE*, Mousa Afrasiabi, Mohammad Amin Jarrahi, Mohammad Mohammadi, *Member, IEEE*, Jamshid Aghaei, *Senior Member, IEEE*, Mohammad Sadegh Javadi, *Senior Member, IEEE*, Miadreza Shafie-Khah, *Senior Member, IEEE*, and João P. S. Catalão, *Senior Member, IEEE*

***Abstract*— Accurate and practical load modeling plays a critical role in the power system studies including stability, control, and protection. Recently, wide-area measurement systems (WAMSs) are utilized to model the static and dynamic behavior of the load consumption pattern in real-time, simultaneously. In this article, a WAMS-based load modeling method is established based on a multi-residual deep learning structure. To do so, a comprehensive and efficient load model founded on combination of impedance–current–power and induction motor (IM) is constructed at the first step. Then, a deep learning-based framework is developed to understand the time-varying and complex behavior of the composite load model (CLM). To do so, a residual convolutional neural network (ResCNN) is developed to capture the spatial features of the load at different location of the large-scale power system. Then, gated recurrent unit (GRU) is used to fully understand the temporal features from highly variant time-domain signals. It is essential to provide a balance between fast and slow variant parameters. Thus, the designed structure is implemented in a parallel manner to fulfill the balance and moreover, weighted fusion method is used to estimate the parameters, as well. Consequently, an error-based loss function is reformulated to improve the training process as well as robustness in the noisy conditions. The numerical experiments on IEEE 68-bus and Iranian 95-bus systems verify the effectiveness and robustness of the proposed load modeling approach. Furthermore, a comparative study with some relevant methods demonstrates the superiority of the proposed structure. The obtained results in the worst-case scenario show error lower than 0.055% considering noisy condition and at least 50% improvement comparing the several state-of-art methods.**

***Index Terms*— Composite load model (CLM), deep learning, gated recurrent unit (GRU), pseudo-Huber loss function, residual convolutional neural network (ResCNN).**

Manuscript received November 6, 2020; revised September 3, 2021 and November 17, 2021; accepted December 4, 2021. *(Corresponding authors: Miadreza Shafie-Khah; João P. S. Catalão.)*

Shahabodin Afrasiabi is with the Department of Electrical and Computer Engineering, University of Saskatchewan, Saskatoon, SK S7N5A9, Canada.

Mousa Afrasiabi and Jamshid Aghaei are with the Department of Electrical Engineering, School of Energy Systems, Lappeenranta University of Technology (LUT), 53850 Lappeenranta, Finland.

Mohammad Amin Jarrahi and Mohammad Mohammadi are with the School of Electrical and Computer Engineering, Shiraz University, Shiraz 71348-14336, Iran.

Mohammad Sadegh Javadi is with the Institute for Systems and Computer Engineering, Technology and Science (INESC TEC), 4200-465 Porto, Portugal.

Miadreza Shafie-Khah is with the School of Technology and Innovations, University of Vaasa, 65200 Vaasa, Finland (e-mail: miadreza@gmail.com).

João P. S. Catalão is with the Faculty of Engineering of the University of Porto (FEUP), 4200-465 Porto, Portugal, and also with the Institute for Systems and Computer Engineering, Technology and Science (INESC TEC), 4200-465 Porto, Portugal (e-mail: catalao@fe.up.pt).

Color versions of one or more figures in this article are available at https://doi.org/10.1109/TNNLS.2021.3133350.

Digital Object Identifier 10.1109/TNNLS.2021.3133350

I. Introduction

A. Motivation

ELECTRICAL load modeling is essential in the analysis of the traditional and reconstructed power systems. In load modeling studies, the main goal is to construct a mathematical description to describe the consumption pattern throughout a specific time interval [1]–[3]. Due to emergence of new concepts such as smart grids, renewable energies, active distribution networks, demand-side management, and so on, electrical load modeling has faced new challenges such as complicated characteristics and random time variance trends [4]–[6]. This study aims to resolve these challenges that still require a comprehensive and general solution. In this regard, the desired approach must have the following features.

1) It must be fast and accurate to track highly variant load characteristics.
2) It must be robust to handle highly noisy conditions.
3) It must have the ability to understand the spatial and temporal features for providing suitable knowledge on load consumption pattern.
4) It must be capable to identify a large number of unknown parameters with regard to the emergence of advanced measurement devices such as phasor measurement units (PMUs) and smart meters provide.

So, the main motivation of this article is to develop a multi-residual deep network to establish a general framework for the wide-area load parameter identification.

B. Brief Literature Review

Load modeling has been conducted in two main stages, including: 1) choosing a proper load model based on measurement-based or physical-based models and 2) designing a parameter estimation approach to identify the selected load model parameters [7], [8]. Physical-based models provide a

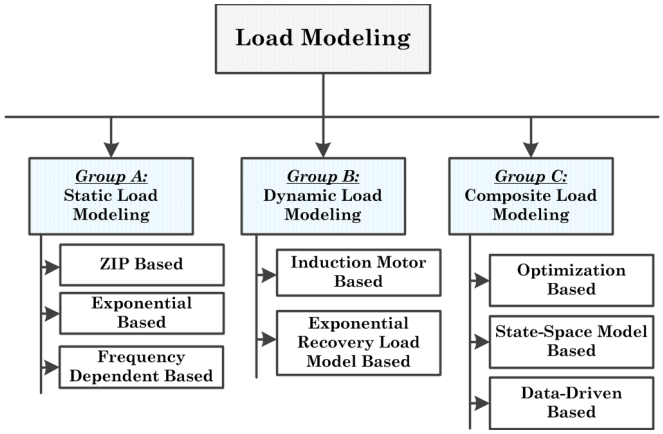

Fig. 1. Load modeling approaches.

detailed description of physical behavior and functioning of electrical devices, however, they are not applicable in practical conditions due to lack of required detailed information [9], [10]. Therefore, measurement-based load models are more preferred as they offer more practical models. The main principle in measurement-based models is collecting a dataset from measurement equipment and directly implemented for load modeling. Based on the behavior, load can be modeled as static type or can be formulated as dynamic model. However, composite models involve the patterns of both static and dynamic models [11].

Fig. 1 presents a classification of load modeling approaches. In this figure, various schemes for each group of load modeling techniques are depicted. The load models in the static category have the ability to represent the active and reactive consumption as the functions of bus frequency and voltage. Several models such as impedance–current–power (ZIP), exponential and frequency-dependent models are most common static load models [12], [13]. Dynamic load models can model the time-variant relationship between active and reactive power based on bus voltage throughout a time interval [14]–[16]. Induction motor (IM) and exponential recovery load model (ERLM) are two widely used dynamic load models in previous literature [17]. However, one single static/dynamic model cannot fully represent a behavior of actual electrical load. Composite load model (CLM) aggregates dynamic and static characteristics which can sufficiently represent the actual load model [18]. Therefore, CLM is one of the most preferable load model in previous studies [19], [20]. To this end, this article proposes an approach to identify parameters of CLM.

In terms of identification approach, the CLM parameter identification approaches can be divided into three following groups: 1) optimization-based techniques; 2) state-space model-based techniques; and 3) data-driven-based approaches. In the following, it is tried to introduce these groups in more detail with the highlights from some papers in each area. The summary of this classification are tabulated in Table I. In this table, the cons and pros of each group are declared.

1) Optimization-Based Techniques: The methods of this group first determine an objective function founded on error that is the difference between measurement and estimated values. Then, they employ different techniques such as Lagrangian-based algorithm [9], particle swarm optimization [21], and heuristic search algorithm [22] to optimize the objective function. The main disadvantages of these approaches are related to high computational complexity and considering only measurement data at current time. As load consumption is a time-series data that depend on the previous time steps, ignoring last data can adversely affect the accuracy.

TABLE I
DESCRIPTIONS OF CLM METHODS

Techniques	References	Attributes (+/-)
Optimization Based	[9], [21], [22]	+ Easy to implement - High computational burden - Considering only data of current time
State-Space Model Based	[23-25]	+ Detailed modeling - Does not consider the correlation between loads - Complicated with huge parameters
Data-Driven Based	[2], [3], [4] [6], [14], [26-28]	+ Highly Adaptive + Does not need load profile - Sensitive to measurement noises

2) State-Space Model-Based Techniques: The approaches in this group attempt to estimate the parameters using measurement data and state-space load model. For instance, a CLM parameter identification is formulated as weighted least-square problem in [23]. Moreover, Kalman filter (KF)-based approaches such as extended KF (EKF) and unscented KF (UKF) are also presented in [24] and [25] for CLM and dynamic load models parameter identification, respectively. Generally, the correlation between the loads of the system at various locations cannot be taken into account in this group. So, this shortcoming considerably affects the performance of the methods. That is why the correlation between loads must be observed in the methods to improve their accuracy.

3) Data-Driven-Based Techniques: Data-driven-based approaches are fast and capable of considering the impact of load at different locations, which are included two main subcategories, that is, shallow and deep structures. The shallow-based structure such as support vector machines (SVMs) [14], artificial neural networks (ANNs) [26], and fuzzy logic [27] are developed in recent years for load parameter estimation. However, these structures are not able to properly realize the nature and characteristics of the measurement raw data. Also, another major shortcoming of these approaches that makes them unusable due to their small hypothesis space is high sensitivity to measurement noise and suffering from lack of generality [28]. Moreover, a large share of previously presented approaches can only utilized for a single bus, and therefore, they are not suitable. Deep learning emergence as an evolutionary concept in machine learning has attended a large number of researchers due to the ability in capturing complex and nonlinear features from the raw time signals [2], [3], [6]. A deep recurrent neural network-based approach, namely long short-term memory (LSTM) is developed in [4]. Although it offers suitable performance, it does not have proper efficiency in learning spatial features and noisy environments. Moreover, single or multimodal LSTM networks are not fully compatible

with different dynamic behaviors for tracking various load patterns.

Considering the presented discussion, this article focuses to present a data-driven-based technique for CLM parameter identification.

C. Contributions

This article, aiming to provide an accurate and fast CLM parameter identification approach, proposes a deep residual-based structure to fully understand robust, spatial, and temporal features. In the designed structure, a convolutional neural network (CNN) is used to realize the spatial features, however, in contrast with RNN-based networks, CNN is weakened to learn spatial features, especially in long-tailed time series associated with high variations. To this end, first a CNN unit converts to residual CNN units and then a gated recurrent unit (GRU) as a time efficient and stronger temporal feature learner than LSTM is added to the designed network. Then, to make a balance between different dynamic behaviors of the load parameter in CLM, the designed network converted into three parallel networks and also improve the computational efficiency. Consequently, an error-based loss function is adopted to improve the method performance in noisy conditions. Furthermore, it can help the method to increase its training ability.

To sum up, the main novelties of the current work are presented as follows.

1) A multi-residual deep network is developed to accurately identify the CLM parameters through strong spatial and temporal learners.
2) An error-based loss function is suggested to enhance the method capability in training process which can provide accurate estimation for CLM parameters in noisy environments.
3) The slow/fast dynamic behavior of CLM parameters are realized using three parallel deep networks, which can improve the time efficiency, as well.

D. Organizations

The organization for the following content is as follows. The mathematical descriptions of the wide-area CLM model are provided in Section II. Section III describes the developed multi-residual deep network in detail. The numerical results and experiments are given in Section IV. At the end, the conclusions are drawn in Section V.

II. Wide-Area Load Modeling

A. Composite Load Model

The CLM involves the static and dynamic components which are modeled as ZIP and IM models, respectively. The ZIP model consists of three main parts which are constant impedance shown as Z, constant current shown as I, and constant power as P, which are formulated as follows [4]:

$$P_t^{\mathrm{ZIP}} = \alpha_t^P \left(\frac{V_t}{V_b}\right)^2 + \beta_t^P \left(\frac{V_t}{V_b}\right) + \gamma_t{}^P \tag{1}$$

$$Q_t^{\mathrm{ZIP}} = \alpha_t^Q \left(\frac{V_t}{V_b}\right)^2 + \beta_t^Q \left(\frac{V_t}{V_b}\right) + \gamma_t{}^Q \tag{2}$$

where P_t^{ZIP} and Q_t^{ZIP} represent active and reactive power in the model, respectively, and $\alpha_t^{P/Q}$, $\beta_t^{P/Q}$, and $\gamma_t{}^{P/Q}$ are constants showing the percentage associated with active/reactive power, subjected to $\alpha_t^{P/Q} + \beta_t^{P/Q} + \gamma_t{}^{P/Q} = 1$, respectively. Based on the ZIP model, the static reflection of loads is dependent on the voltage variation.

The dynamic component of the CLM is formulated as a three-order IM model with taking into account of the meteorological impacts and consuming load patterns [11]

$$\dot{v}_d^t = \frac{-r_R^t}{x_R^t + x_m^t}\left(v_d^t + \frac{\left(x_m^t\right)^2}{x_m^t + x_R^t} i_q^t\right) + s^t v_q^t \tag{3}$$

$$\dot{v}_q^t = \frac{-r_R^t}{x_R^t + x_m^t}\left(v_q^t + \frac{\left(x_m^t\right)^2}{x_m^t + x_R^t} i_d^t\right) + s^t v_d^t \tag{4}$$

$$\dot{s}^t = \frac{1}{2H^t}\left(T_m\left(1 - s^t\right)^2 - v_d^t i_d^t - v_q^t i_q^t\right) \tag{5}$$

where $v_{d/q}^t$ and s^t show d/q-axis transient voltage and rotor slip as state variables, while parameters r_R^t, x_R^t, x_m^t, H^t, and T_m represent rotor resistance, rotor reactance, magnetizing reactance, motor inertia, and mechanical torque, respectively. The IM model is described by voltage, current, and slip of IM as the state variables, while the parameters need to be identified are resistance/reactance of the stator/rotor, motor inertial, and magnetizing reactance.

In addition, d/q-axis stator currents are shown by $v_{d/q}^t$ and computed, as

$$i_d^t = \frac{r_S^t\left(u_d^t - v_d^t\right) + x_{\mathrm{sc}}^t\left(u_q^t - v_q^t\right)}{\left(r_S^t\right)^2 + \left(x_{\mathrm{sc}}^t\right)^2} \tag{6}$$

$$i_q^t = \frac{r_S^t\left(u_q^t - v_q^t\right) + x_{\mathrm{sc}}^t\left(u_d^t - v_d^t\right)}{\left(r_S^t\right)^2 + \left(x_{\mathrm{sc}}^t\right)^2} \tag{7}$$

where d/q-axis bus voltage, stator resistance, and short-circuit reactance are, respectively, depicted by $u_{d/q}^t$, r_s^t, and x_s^t. The measured bus voltage V_b^t consists of d and q-axis components, as $\left(V_b^t\right)^2 = \left(u_d^t\right)^2 + \left(u_q^t\right)^2$. Furthermore, x_{sh}^t obtains algebraically, as

$$x_{\mathrm{sh}}^t = x_S^t + \frac{x_m^t x_R^t}{x_m^t + x_R^t}. \tag{8}$$

The consuming active and reactive power of the IMs as time-varying parameters is modeled as

$$P_{\mathrm{IM}}^t = \frac{\left\{r_S^t\left[\left(u_d^t\right)^2 + \left(u_q^t\right)^2 - u_d^t v_d^t - u_q^t v_q^t\right] - x_{\mathrm{sh}}^t\left(u_d^t v_q^t - u_q^t v_d^t\right)\right\}}{\left[\left(r_s^t\right)^2 + \left(x_{\mathrm{sh}}^t\right)^2\right]} \tag{9}$$

$$Q_{\mathrm{IM}}^t = \frac{\left\{x_{\mathrm{sh}}^t\left[\left(u_d^t\right)^2 + \left(u_q^t\right)^2 - u_d^t v_d^t - u_q^t v_q^t\right] - r_s^t\left(u_d^t v_q^t - u_q^t v_d^t\right)\right\}}{\left[\left(r_s^t\right)^2 + \left(x_{\mathrm{sh}}^t\right)^2\right]}. \tag{10}$$

Consequently, the consuming active and reactive power in the CLM are

$$P^t_{\text{com}} = P^t_{\text{ZIP}} + P^t_{\text{IM}} \tag{11}$$
$$Q^t_{\text{com}} = Q^t_{\text{ZIP}} + Q^t_{\text{IM}}. \tag{12}$$

B. Conventional Load Parameter Identification

To estimate the time-varying load parameters, two sets of parameters including load and measurable variables are considered which denoted as Θ^t_d and Υ^t_d, respectively. In this regard, these parameters are $\Theta^t_{d^\Theta} = \left[r^t_S, x^t_S, x^t_m, x^t_R, r^t_R, H^t, \alpha^P_t, \alpha^Q_t, \beta^P_t, \beta^Q_t\right]$ and $\Upsilon^t_{dY} = \left[P^t_{\text{com}}, Q^t_{\text{com}}, V^t_b\right]$. The dimension of CLM and measured parameters by WAMS are, respectively, represented by d^Θ and d^Υ.

Overall, the CLM shows a function depended on the measured variables associated with measurement/process noises, $\Theta^t_{d^\Theta} = f\left(\Upsilon^{tr}_d\right) + e_\Upsilon$.

In the k time interval, CLM parameters can be as follows:

$$\Theta^t_{d^\Theta} = \Theta^{t-1}_{d^\Theta} + e_{\Theta^1} = \Theta^{t-2}_{d^\Theta} + e_{\Theta^2} = \cdots = \Theta^{t-k_\Theta}_{d^\Theta} + e_{\Theta^{k_\Theta}} \tag{13}$$

where k_Θ represent the estimation time horizon of CLM parameters. Similarity, the dependency of CLM parameters and measurement variables can be described as

$$\Theta^t_{d^\Theta} = f\left(\Upsilon^t_d\right) + e_Y = f_1\left(\Upsilon^{t-1}_d\right) + e_{Y^1} = \cdots = f_{k_Y}\left(\Upsilon^{t-k_Y}_{d'}\right) + e_{Y^{k_Y}} \tag{14}$$

where k_Υ is a window length of measurement.

C. Wide-Area Load Parameter Identification

From the practical point of view, wide-area load modeling is carried out based on the wide-area measurement systems. First, the information in the whole power system should be send to the centralized control center. Then, the control center organized the received data as an input for the designed data-driven-based load parameter identification block. The input data activates the trained network. Formerly, the load parameters of the system are estimated by the designed network. The mentioned procedure is shown in Fig. 2.

The correlation of the electrical load consumption has taken into account in the load parameter identification via WAMS. Therefore, CLM load models are described based on $F^t_{d_Y}$ as

$$\chi^t_{d_\chi,i} = F^t_{d_Y}\left(\chi^t_{d_{\chi,1}}, \ldots, \chi^t_{d_{\chi,N}}\right). \tag{15}$$

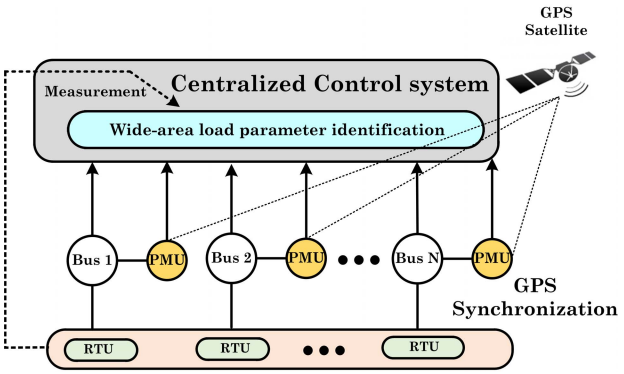

Fig. 2. Overall schematic on the practical implementation of the wide-area measurement-based load parameter identification.

The bus number is represented by i, while N depicts the total number of the buses in the network.

Considering (14) and (15), CLM based on WAMS can be formulated as (16), shown at the bottom of the page, [4], where $\Theta_{d^\Theta \times k_\Theta}$, $\chi_{d_\chi \times (k_\Upsilon+1)}$, and $\chi_{d_\chi \times (k_\Upsilon+1)}$ are written, respectively, as

$$\Theta_{d^\Theta \times k_\Theta} = \left(\Theta^{t-1}_{d^\Theta}, \Theta^{t-2}_{d^\Theta}, \ldots, \Theta^{t-k_\Theta}_{d^\Theta}\right) \tag{17}$$
$$\chi_{d_\chi \times (k_{\Upsilon+1})} = \left(, \ldots, \chi_{d_\chi \times (k_\Upsilon+1),i}, \ldots, \chi_{d_\chi \times (k_{\Upsilon+1}),N}\right) \tag{18}$$
$$\chi_{d_\chi \times (k_Y+1),i} = \left(\chi^t_{d_\chi,i}, \chi^{t-1}_{d_\chi,i}, \ldots, \chi^{t-k_Y}_{d_{\chi,i}}\right). \tag{19}$$

An analytical model cannot estimate the parameter in (16), and therefore, this article proposes a data-driven method to identify the time-varying parameters.

III. Wide-Area CLM Modeling Based on Multi-Task Deep Learning Approach

In the data-driven load modeling, historical data including $\Theta_{d^\Theta \times k_\Theta, i} \in \mathbb{R}^{d^\Theta \times k_\Theta}$ and $\chi_{d_\chi \times (k_Y+1)} \in \mathbb{R}^{d_\chi \times (k_Y+1)}$ is the basis to approximate a function with the output of $\Theta'_{d^\Theta \times k_\Theta, i} \in \mathbb{R}^{d^\Theta \times k_\Theta}$. The data-driven structure should be able to generate the output with a minimum difference between $\Theta_{d^\ominus \times k_\Theta, i}$ and $\Theta'_{d^\ominus} \times k_\Theta, i$. The input dataset is defined as $X = \left\{\left(\Theta^{t-k_\Theta}_d, \ldots, \Theta^{t-1}_d\right), \left(\chi^{t-k_Y}_{d_y,i}, \chi^{t-1}_{d_\chi,i}\right)\right\}$ and the output is $Y = \left\{\left(\Theta'^t_{d^\theta}\right)\right\}$ in the data-driven load parameter estimation. To design a structure to estimate CLM parameters, the squared error loss function is usually used.

The conventional loss function is a squared error loss function. The main shortcoming of this loss function is the possibility of mean biased or estimation of minimum variance. To address this issue, this article reformulates the loss function

$$\Theta^t_{d^\Theta} = \mathcal{F}_\chi\left(\underbrace{\underbrace{\Theta^{t-1}_{d^\Theta}, \ldots, \Theta^{t-k_\Theta}_{d^\Theta}}_{\Theta_{d^\Theta \times k_\Theta}}, \ldots, \underbrace{\chi^t_{d_\chi.1}, \ldots, \chi^{t-k_\Upsilon}_{d_\Upsilon.1}}_{\chi_{d_\chi \times (k_\Upsilon+1).1}} \cdot \underbrace{\chi^t_{d_\chi.2}, \ldots, \chi^{t-k_\Upsilon}_{d_\Upsilon.0}}_{\chi_{d_\chi \times (k_\Upsilon+1).2}}, \ldots, \underbrace{\chi^t_{d_\chi.N}, \ldots, \chi^{t-k_\Upsilon}_{d_\Upsilon.N}}_{\chi_{d_\chi \times (k_\Upsilon+1).N}}}_{\chi_{d_\chi \times (k_\Upsilon+1)}}\right) \tag{16}$$

with a novel approach entitled as pseudo-Huber loss function as follows [29]:

$$f_{\text{loss}}^{pH}(Y) = \sum_{t=1}^{T}\left[C^2\sqrt{\frac{c^2+(\mathrm{Y}_t)^2}{C^2}}\right] - C^2 \tag{20}$$

where f_{loss}^{pH} represents the loss function and control parameter, respectively. This loss function outputs the values lose to $(Y)^2/2$. Therefore, it is prevented the large values due to producing the straight line with the slope $(Y)^2/2$. Furthermore, the performance of the suggested loss function would not be significantly affected by external factors including noises. Thus, the learning weights θ_l of each lth layer can be obtained as

$$\theta_l^{pH}(X) = \frac{\theta_l(X)}{\sqrt{1+\left(\frac{\tilde{Y}_{pH}-Y_l}{C}\right)^2}}. \tag{21}$$

Moreover, the estimator of the proposed pseudo-Huber loss function, $\tilde{Y}_{pH}$, is defined as follows:

$$\tilde{Y}_{pH} = \frac{\sum_{t=1}^{T}\theta_l^{pH}(X)Y_l}{\sum_{t=1}^{T}\theta_l^{pH}(X)}. \tag{22}$$

The efficient and well-known gradient descent-based Adam [30], [31] is utilized to find the optimal learning weights. That is why, the developed loss function have high degree of robustness against various noises such as measurement and process ones in CLM.

Although a loss function plays a key role in designing a strong approach in time-varying CLM, it is essential to design a network that can understand spatio-temporal features of time signals in the power systems. Thus, this article presents a multi-task residual spatio-temporal deep consists of three parallel parts and each part consists of four main blocks, that is, residual CNN, GRU, fully-connected networks (FCNs), and weight fusion blocks. The proposed structure is depicted in Fig. 3.

A. Arrangement of Input Dataset

In the first step, the measurement and load parameters obtained by a generated dataset is normalized based on [32]

$$X^i = \frac{x^i - X^i_{\min}}{X^i_{\max} - X^i_{\min}} \tag{23}$$

the maximum and minimum input values are shown as $X^i_{\max}$ and $X^i_{\min}$, respectively.

The 1-D time series is not sufficient for complete feature extraction. Therefore, the representation learning technique is applied in which the initial dataset, which is extensively assessed using real input, is converted to 2-D vectors through the following [33]:

$$X^i = \begin{bmatrix} \Theta_d^{t-1} & \chi_{d_\chi^{-1}}^{t-1} \\ \Theta_{d^\Theta}^{t-2} & \chi_{d_\chi^{t-2}}^{(\Theta)} \\ \vdots & \vdots \\ \Theta_{d^\Theta}^{t-k_\Theta} & \chi_{d_\chi}^{t-k_\Upsilon} \end{bmatrix}. \tag{24}$$

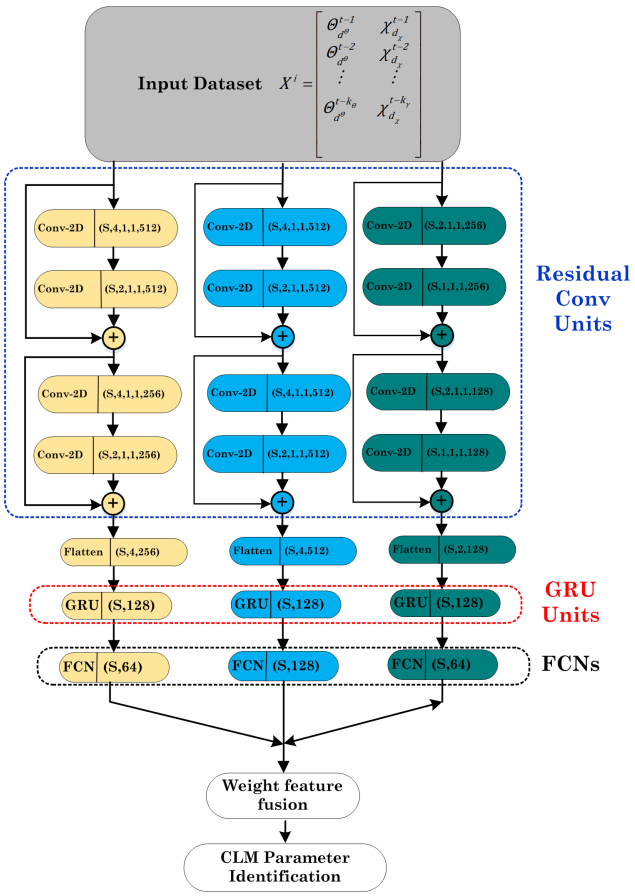

Fig. 3. Proposed multi-residual deep network structure for CLM parameter estimation.

B. Residual CNN

In the first blocks of the designed deep network, raw data is fed into a CNN block. The measurement and parameter data in the previous time intervals construct a sparse and noisy input dataset. In the first block, convolutional layers and max-polling layers are used to extract time-varying patterns and spatial dependency between measurement signals from different buses in the power system. The convolutional layers consist of multiple kernels with a size of $\underbrace{wi}_{\text{width}} \times \underbrace{he}_{\text{height}}$. The output of lth convolution layer is as follows [34]:

$$O_{l,i}^{\text{Conv}} = f^{act}\left(\omega_{l,i}^{\text{Conv}} \otimes X_i + B_{l,i}\right) \tag{25}$$

where $O_{l,i}^{\text{Conv}}$, $\omega_{l,i}^{\text{Conv}}$, and $B_{l,i}$ represent the output, weight matrix, and bias matrix of the lth convolutional layer, respectively. Also, the function f^{act} and the operator $\otimes$ show activation function and convolutional operator, respectively. As can be seen from (25), the input measurement and load parameters are filtered based on the activation function for the several times. Also, the input data convolved to extract the inherent features including spatial features (loads at different locations).

To enhance the CNN performance in capturing spatial features, we added a residual mapping after two convolutional layers, and therefore, the output after passing through a

residual network is

$$O_i^{\text{res}} = f^m + X_i^{\text{res}} \tag{26}$$

where the output of the residual unit, mapping element, and input of the residual units are shown by O_i^{res}, f^m, and X_i^{res}, respectively.

C. Gated Recurrent Unit

In the second blocks of three parallel structures, GRU units are added to the designed multi-residual deep network to capture fully temporal feature as a time-efficient version of memory-based recurrent neural networks. GRU units as the modified version of LSTM consist of update and reset gates. The update gate stores the important features throughout a signal and realize long-term dependency, while rest gate removes features with low weight importance by resetting memory [3].

D. Fully-Connected Networks

The FCN layers are used to control the dimension of the GRU, the three parallel FCN layers are trained in an end-to-end manner, and improve the training performance without further machinery [34].

E. Weighted Fusion Block

In the time-varying composite model, different parameters in static and dynamic models have a different impact on the parameter identification performance. For example, in ZIP load model, the parameters might be almost constant, in particular, during the normal operational conditions, while dynamic parameters could highly change during an ultra-short-term period, such in the millisecond time period. Thus, different influential factors could highly influence on the parameter estimation with different behavior [35]. To this end, first we designed a three parallel networks, and then a fusion method is used to construct final outputs as

$$O^{\text{fu}} = \omega^{P_1} \odot O^{P_1} + \omega^{P_2} \odot O^{P_2} + \omega^{P_3} \odot O^{P_3} \tag{27}$$

where O^{fu}, $\omega^{P_1/P_2/P_3}$, and $O^{P_1/P_2/P_3}$ show the output of weight fusion block, each parallel part of the designed multi-residual network weights and outputs, respectively. The output of weight fusion block is the final output of the proposed deep approach for CLM parameters $\Theta_d'^t$ with the aim of minimum difference with the aim of minimum difference with Θ_d^t.

F. Training Process

The training process is given in Fig. 4. As can be seen, training of the designed deep learning-based CLM parameter identification is simple. First, the designed network is fed by a set of historical data, and then an iterative process is conducted to obtain a set of optimal learning weights by optimizing a pseudo-Huber loss function and Adam algorithm.

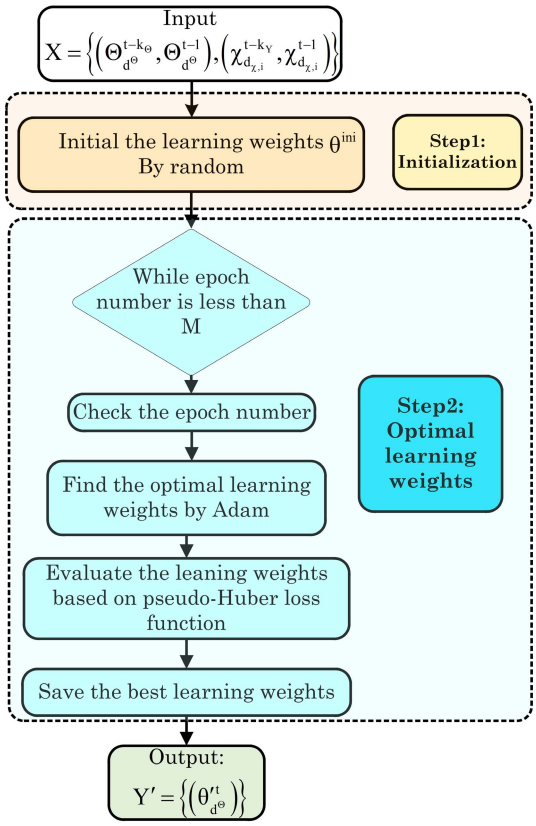

Fig. 4. Training process of the multi-residual deep network.

G. Design Procedure

To provide a balance between the slow and fast variants in the CLM parameters identification, the designed structure composes of three parallel branches as follows.

1) The first branch is trained based on the measurement parameters and parameters of the ZIP model $\left(\alpha_t^P, \beta_t^P, \alpha_t^Q \cdot \alpha_t^Q\right)$.
2) The second branch is trained using measurement parameters, rotor, and stator parameters of the IM $\left(x_S^t, x_R^t, r_S^t, r_r^t\right)$.
3) The last branch is trained based on the H^t and x_m^t.

As can be seen from Fig 1, each branch includes two residual CNNs, one GRU, and one FCN layer. To this end, the proposed network is designed based on the following steps.

1) *Step 1:* Initialization.

Step 1.1: The input data (measurement and parameters) is normalized based on (23).

Step 1.2: The normalized data is converted from 1-D to 2-D signals.

2) *Step 2:* Residual CNN.

Step 2.1: As mentioned above, three parallel blocks have been considered to provide a balance between the slow and dynamic behavior of the parameters in the static and dynamic models. Each block consists of two residual CNNs and the first convolutional layer converts the input to (S,4,1,1,512) (S: samples) into the two parallel branches and the output of the last branch (including measurement data and historical data of H^t and x_m^t) form is (S,2,1,1,512). Furthermore, about

15% of the layers are dropped out in the first residual CNN layers. The dropout approach is a beneficial and widely used technique to prevent overfitting as well as improve the computational burden of the designed network. *Step 2.2*: In the second residual CNN, the output of the first residual CNN converts to the outputs with sizes (S,2,1,1,512) into the two parallel layers (including IM rotor, IM stator, and ZIP parameters), while the form of the outputs in the last parallel layer is (S,2,1,1,512). In the second residual CNN layers, about 25% of the layers are dropped.

3) *Step 3:* GRU.

Step 3.1: The outputs of residual CNN blocks are 2-D signals. First, 2-D signals convert to the 1-D signals by using a flatten layer. Therefore, flatten layers are used to convert 2-D signals to 1-D signals with the size of (S,4,256), (S,4,512), and (S,2,218) in the first, second, and third parallel layers.

Step 3.2: The 1-D outputs of flattening layers are fed into the three sets of GRU layers, each branch consisting of one of the GRU layers. The output of GRU layers is the time series with the size of (S,128).

4) *Step 4:* FCN.

Step 4.1: The output of GRU is fed into the FCN blocks. FCN block converts the outputs of GRU into the vectors with a size of (S,64), (S,128), and (S,64) in the first, second, and third parallel layers, respectively.

5) *Step 5:* Output.

Step 5.1: The outputs of the FCN blocks are fed into the weight fusion block. The weight fusion block is used to concatenate the three parts and then construct the final outputs. These outputs are the results of CLM parameter identification.

IV. Numerical Experiments

The numerical results of the designed deep-based CLM parameter identification structure are given in this section. The robustness and effectiveness of the proposed multi-residual deep network are validated using two benchmark case studies with regard to noise impacts. For the sake of the comparison, four different data-driven approaches including multi-LSTM [4], single LSTM [4], and 1-D-CNN [36] as previously presented deep networks and SVM [14] as shallow-based networks have been considered. Besides, to show the GRU unit's impacts on the performance of the proposed approach, we consider the designed network without GRU units and as a state-of-the-art approach, multi-residual convolutional (MRC) approach is also used for assessing the performance of the developed technique.

The designed network is coded in Python (TensorFlow package) and the two datasets are gathered from MATLAB program in a PC system with Core I7 CPU @3.00 GHz RAM.

A. Data Generation and Description

The first benchmark system considered for this study is IEEE 68-bus system. This system involves 86 lines and 16 generators. To simulate the network, the power system toolbox (PST) with 0.01 samples per second has been utilized [37]. Two methods are deliberated to generate the datasets. To illustrate the generation technique with an example, consider that the IEEE 68-bus system has 34 different loads which are disconnected from the system each a time, while the data is recorded. Then, this trend is taken into account for the lines. In other words, they also disconnected from the system while the data is being captured. This procedure leads to generating more than 59 500 various samples from the IEEE 68-bus system. This obtained data is divided into three subsections including training, validation, and testing samples. In this regard, 70% of the data is assigned to training stage, while 15% of samples are considered for the validation and the remaining 15% of this dataset is devoted to the testing process. It must be noted that the noisy data is generated based on Normal distribution function with the mean values equaled to mean values of original data and standard deviation equaled to 10% of the mean values. These produced noisy samples are also considered in the evaluation of the developed technique.

B. Evaluation Metrics

Four important and critical error-based metrics are considered to assess the performance of the designed network from numerical aspects. The formulation of these indices is brought as follows.

1) Root mean square error (RMSE)

$$\mathrm{RMSE} = \sqrt{\frac{1}{N}\sum_{i=1}^{N}\left(Y_i' - Y_i\right)^2}. \tag{28}$$

2) Normalized root mean square error (NRMSE)

$$\mathrm{NRMSE} = \frac{1}{Y_i^{\max}}\sqrt{\frac{1}{N}\sum_{i=1}^{N}\left(Y_i' - Y_i\right)^2}. \tag{29}$$

3) Mean absolute error (MAE)

$$\mathrm{MAE} = \frac{1}{N}\sum_{i=1}^{N}\left|Y_i' - Y_i\right|. \tag{30}$$

4) Mean absolute percentage error (MAE)

$$\mathrm{MAPE} = \frac{1}{N}\sum_{i=1}^{N}\left|\frac{Y_i' - Y_i}{Y_i}\right|. \tag{31}$$

C. Discussion on Results

Figs. 5 and 6 show the comparative results of the proposed method (PM) with the actual values and estimated parameters by the MCR approach. In these figures, it can be seen that the proposed approach follows the pattern of measured α_p^t and x_m^t with high degree of accuracy. These results indicate that the proposed approach has high capabilities in this regard.

The performance of the proposed approach in terms of four different accuracy indices with regard to the defined equations (28)–(31) is given in Fig. 7. As can be seen from this figure, the results validate the high accuracy of the proposed approach.

The comparative study between the mentioned methods and the suggested technique for the estimation of α_p^t and x_m^t are given in Figs. 8 and 9. From these figures, it is clear that the proposed approach is far more accurate than the

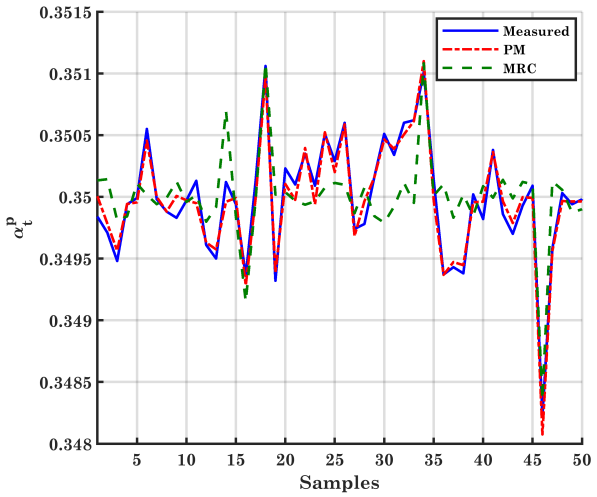

Fig. 5. Estimation results of α_t^p obtained by PM and MRC approaches versus actual data.

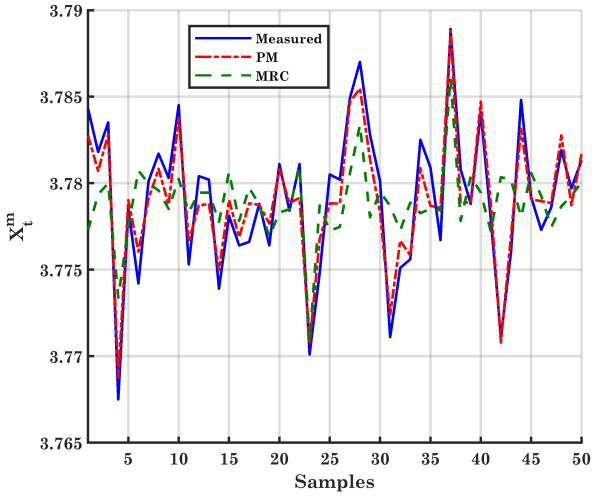

Fig. 6. Estimation results of x_t^m obtained by PM and MRC approaches versus actual data.

state-of-the-art approaches. For instance, based on Fig. 8, the proposed approach has a higher accuracy percentage in terms of MAPE than MRC, MLSTM, LSTM, 1-D CNN, and SVM which are 73.14%, 77.70%, 90.42%, 93.73%, and 98.35%, respectively. Also, Fig. 9 denotes that the developed scheme is more accurate in terms of NRMSE than SVM which its performance is 94.80%. Also the developed scheme has a better performance than MLSTM, LSTM, and 1-D CNN which have approximately 76.50%, 89.51%, and 89.63% percentage in terms of NRMSE, respectively. The comparison between the proposed approach and MRC shows the effectiveness of the GRU units with improving accuracy significantly, about 74.20% and 69.24% based on NRMSE values in estimation of parameters, α_p^t and x_m^t, respectively.

D. Sensitivity Analysis on Parallel Structure

To analyze the effectiveness of the proposed approach with different parallel parts, a sensitivity study is conducted. The

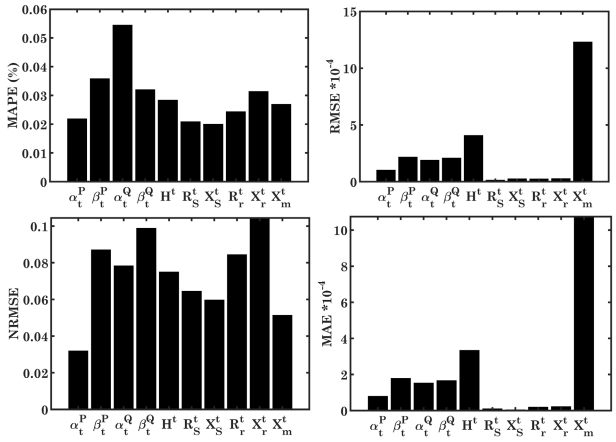

Fig. 7. Obtained metrics by the PM in wide-area load modeling.

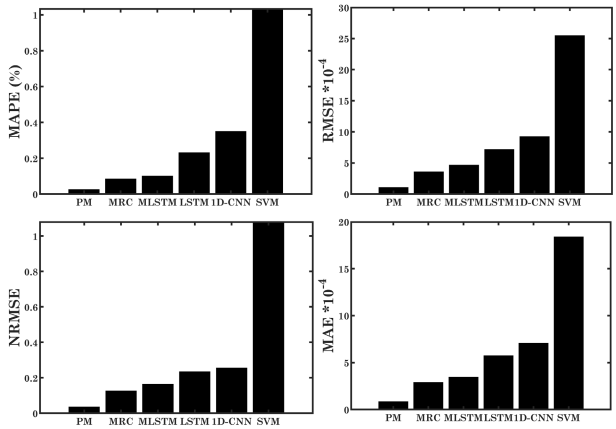

Fig. 8. Estimation results of α_t^p obtained by PM in parameter identification of CLM with MRC, MLSTM, LSTM, 1-D CNN, and SVM schemes.

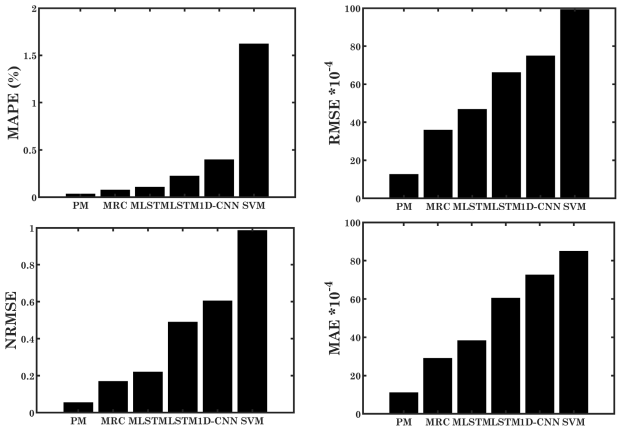

Fig. 9. Estimation results of x_t^m obtained by PM in parameter identification of CLM with MRC, MLSTM, LSTM, 1-D CNN, and SVM schemes.

results of time-varying load parameter identification for parameter x_m^t are depicted in Fig. 10 with regard to the mentioned four different indices. As can be realized, the performance of the proposed approach with three different parts is more accurate than the scheme with one, two, four, and five parts.

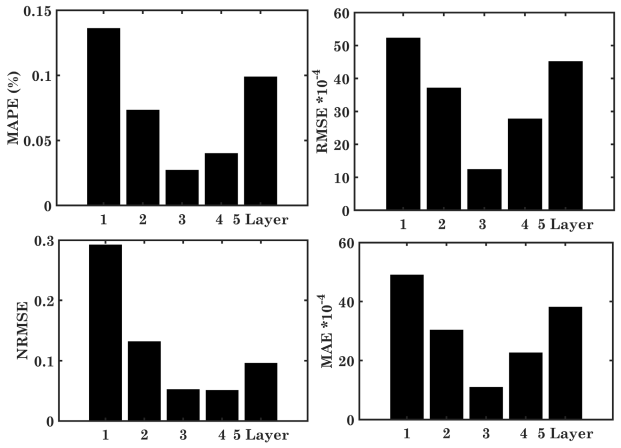

Fig. 10. Comparison of different structures of the PM in parameter identification of CLM with 1–5 parallel layers in estimation of x_t^m.

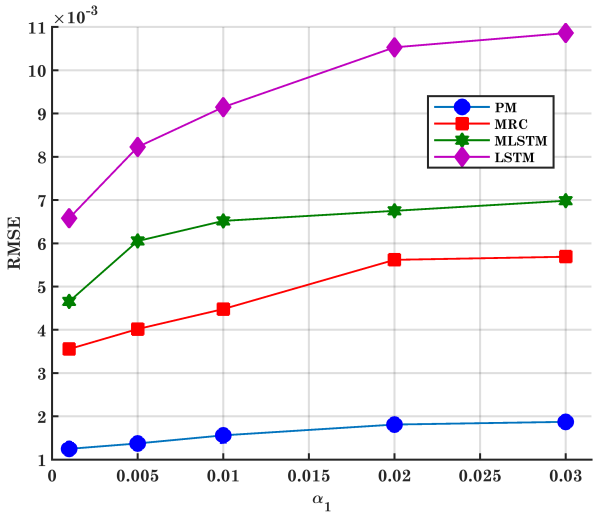

Fig. 11. Proposed multi-residual deep network structure for CLM parameter. Comparison of the PM, MRC, MLSTM, and LSTM results on x_t^m estimation in terms of RMSE.

With increasing number of the parts from one to three, the accuracy is enhanced. However, the designed deep network with five different parts shows lower accuracy than with three and four parts. For example, the proposed approach with three parallel layers is significantly reduced the error in terms of MAPE associated with one, two, four, and five parallel layers approximately 80.32%, 63.37%, 32.41%, and 72.83%, respectively. It can be stated that the higher number of parallel branches leads to overfitting.

E. Sensitivity Analysis on Noise

The robustness of the proposed approach is discussed in this section through a comparison with other approaches. To this end, five different noise signals are added to the actual values; each of them follows a Gaussian distribution with zero mean and standard deviation of 0.005, 0.01, 0.015, 0.02, 0.025, and 0.03 (shown by α_1). Figs. 11 and 12 compared the results for estimation of x_m^t obtained by the proposed approach, MRC, MLSTM, and LSTM in terms of RMSE and MAPE

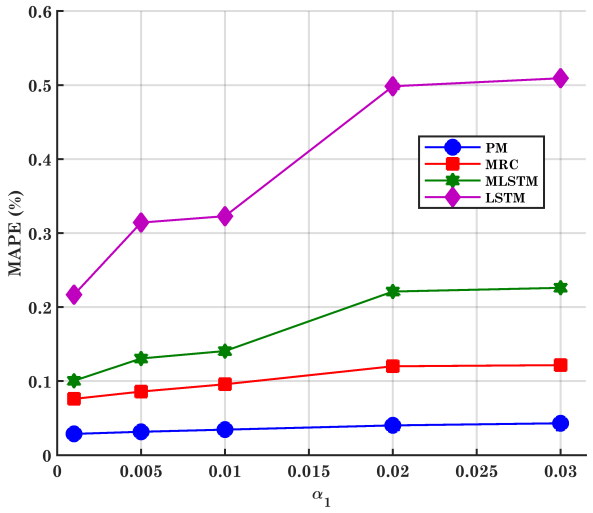

Fig. 12. Proposed multi-residual deep network structure for CLM parameter. Comparison of the PM, MRC, MLSTM, and LSTM results on x_t^m estimation in terms of MAPE.

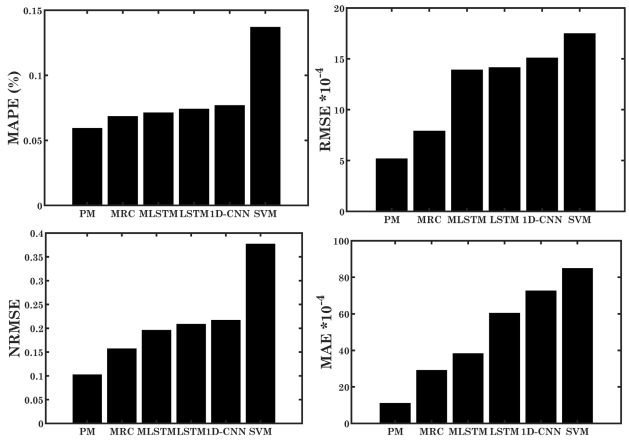

Fig. 13. Estimation results of H^t obtained by PM in parameter identification of CLM with MRC, MLSTM. LSTM, 1-D CNN, and SVM schemes in Iranian 95-bus system.

indices. As can be seen, the proposed approach is far more accurate than other approaches and the results demonstrated the robustness of the proposed approach in noisy conditions. For instance, in highly noise condition with standard deviation 0.03, the proposed approach is more accurate than MRC, MLSTM, and LSTM, about 64.61%, 80.91%, and 86.91%, respectively, based on Fig. 11. From Fig. 12, it is clear that MAPE of the designed network, MCR, MLSTM, and LSTM are 0.001872, 0.005689, 0.006983, and 0.01086, respectively, in highly noise condition ($\alpha_1 = 0.03$). These MAPE value shows that the proposed approach has improved accuracy of multi-residual CNN-based CLM parameter identification significantly, about four times better. Besides, the error of the proposed approach in estimation of x_m^t are at least five and seven times less than MLSTM and LSTM, respectively.

F. Further Results: Iranian 95-Bus Network

To verify the generality of the PM, the real network of Iranian 95-bus network is considered [38]. To this end, the proposed approach is tested on the data gathered from this

network, in which the results obtained by the proposed network on the estimation of the H^t of the load connected to the bus 63 (more information is provided in [38]). The results are compared based on some metrics shown in Fig. 13. As can be seen, it is clear that the designed multi-residual deep network is superior over the compared methods. Therefore, based on attained results on the IEEE-68 bus system and Iranian 95-bus systems, the effectiveness as well as generality of the proposed approach is demonstrated.

V. Conclusion and Future Works

In the power system studies, it is essential to model the loads with highest accuracy to achieve more precise results. The proper load modeling procedure has two consecutive stages which are a selecting practical load model and developing a powerful parameter identification scheme. In this article, the wide-area CLM is selected as a realistic and practical load model. Furthermore, a fast and accurate deep neural network, namely multi-residual deep neural network, is designed to achieve the unknown parameters. The proposed approach benefits from a residual convolutional layer to capture spatial and robust features of the measurement signal and used GRU unit to realize fully temporal features. To make a balance between learning dynamic and static behavior of CLM parameters, the proposed network is designed in three parallel manners. The training ability and noise immunity of the designed technique is boosted by a reformulated error loss function named pseudo-Huber loss function. The methodology is assessed on two different case studies including IEEE 68-bus and Iranian 95-bus. The results network verifies the superiority of the proposed approach through comparison with previous approaches such as MLSTM, LSTM, and SVM, with at least more than 70% accuracy improvement. To address the GRU application in the designed network, the proposed approach is compared with MCR (the proposed approach without GRU units) and shows at least 50% accuracy improvement. The sensitivity analysis on noise shows that the proposed network is almost robust in different noisy conditions and shows at least three times less error compared with other approaches. Finally, a three parallel structures efficiency is demonstrated by a comparative analysis with different structure of the designed network.

The investigations on the proposed CLM parameter estimation based on WAMS reveal that further explorations in the following directions would be worthwhile.

1) Estimation of the full statistical information of the electrical loads from the probability density function (pdf) instead of point estimations of load parameters.
2) Developing parameter identification models for composite demand side models such as combination of load, renewable power generations, and energy storage devices. In this case, the number of the parameters and the model would change and the uncertainty associated with renewable generations can be a serious challenge in the modern power systems.

References

[1] A. Arif, Z. Wang, J. Wang, B. Mather, H. Bashualdo, and D. Zhao, "Load modeling—A review," *IEEE Trans. Smart Grid*, vol. 9, no. 6, pp. 5986–5999, Nov. 2018.

[2] X. Wang, Y. Wang, D. Shi, J. Wang, and Z. Wang, "Two-stage WECC composite load modeling: A double deep Q-learning networks approach," *IEEE Trans. Smart Grid*, vol. 11, no. 5, pp. 4331–4344, Sep. 2020.

[3] F. Bu, Z. Ma, Y. Yuan, and Z. Wang, "WECC composite load model parameter identification using evolutionary deep reinforcement learning," *IEEE Trans. Smart Grid*, vol. 11, no. 6, pp. 5407–5417, Nov. 2020.

[4] M. Cui, M. Khodayar, C. Chen, X. Wang, Y. Zhang, and M. Khodayar, "Deep learning-based time-varying parameter identification for system-wide load modeling," *IEEE Trans. Smart Grid*, vol. 10, no. 6, pp. 6102–6114, Nov. 2019.

[5] Z. Ma, B. Cui, Z. Wang, and D. Zhao, "Parameter reduction of composite load model using active subspace method," *IEEE Trans. Power Syst.*, vol. 36, no. 6, pp. 5441–5452, Nov. 2021.

[6] M. Khodayar and J. Wang, "Probabilistic time-varying parameter identification for load modeling: A deep generative approach," *IEEE Trans. Ind. Informat.*, vol. 17, no. 3, pp. 1625–1636, Mar. 2021.

[7] Y. Lin, Y. Wang, J. Wang, and D. Shi, "Tensor-based parameter reduction of dynamic load models with variable frequency drive," *IEEE Trans. Power Syst.*, early access, Jul. 29, 2021, doi: 10.1109/TPWRS.2021.3100563.

[8] G. Dudek, P. Pelka, and S. Smyl, "A hybrid residual dilated LSTM and exponential smoothing model for midterm electric load forecasting," *IEEE Trans. Neural Netw. Learn. Syst.*, early access, Jan. 8, 2021, doi: 10.1109/TNNLS.2020.3046629.

[9] M. Kabiri and N. Amjady, "A hybrid estimation and identification method for online calculation of voltage-dependent load parameters," *IEEE Syst. J.*, vol. 13, no. 1, pp. 792–801, Mar. 2019.

[10] C. Zheng *et al.*, "A novel equivalent model of active distribution networks based on LSTM," *IEEE Trans. Neural Netw. Learn. Syst.*, vol. 30, no. 9, pp. 2611–2624, Sep. 2019.

[11] J.-K. Kim *et al.*, "Fast and reliable estimation of composite load model parameters using analytical similarity of parameter sensitivity," *IEEE Trans. Power Syst.*, vol. 31, no. 1, pp. 663–671, Jan. 2016.

[12] C. Wang, Z. Wang, and S. Ma, "SVM-based parameter identification for static load modeling," in *Proc. IEEE/PES Transmiss. Distrib. Conf. Expo. (TD)*, Apr. 2018, pp. 1–5.

[13] Y. Lin, Y. Wang, J. Wang, S. Wang, and D. Shi, "Global sensitivity analysis in load modeling via low-rank tensor," *IEEE Trans. Smart Grid*, vol. 11, no. 3, pp. 2737–2740, May 2020.

[14] C. Wang, Z. Wang, J. Wang, and D. Zhao, "SVM-based parameter identification for composite ZIP and electronic load modeling," *IEEE Trans. Power Syst.*, vol. 34, no. 1, pp. 182–193, Jan. 2019.

[15] A. Ellis, D. Kosterev, and A. Meklin, "Dynamic load models: Where are we?" in *Proc. Transmiss. Distrib. Conf. Exhib. (PES)*, Brightun, U.K., 2006, pp. 1320–1324.

[16] E. O. Kontis, T. A. Papadopoulos, A. I. Chrysochos, and G. K. Papagiannis, "Measurement-based dynamic load modeling using the vector fitting technique," *IEEE Trans. Power Syst.*, vol. 33, no. 1, pp. 338–351, Jan. 2018.

[17] X. Zhang, D. J. Hill, and C. Lu, "Identification of composite demand side model with distributed photovoltaic generation and energy storage," *IEEE Trans. Sustain. Energy*, vol. 11, no. 1, pp. 326–336, Jan. 2020.

[18] Q. Huang *et al.*, "A generic modeling and development approach for WECC composite load model," *Electr. Power Syst. Res.*, vol. 172, pp. 1–10, Jul. 2019.

[19] S. Yu, S. Zhang, and X. Zhang, "Two-step method for the online parameter identification of a new simplified composite load model," *IET Gener., Transmiss. Distrib.*, vol. 10, no. 16, pp. 4048–4056, 2016.

[20] M. E.-N. Jahromi and M. T. Ameli, "Measurement-based modelling of composite load using genetic algorithm," *Electr. Power Syst. Res.*, vol. 158, pp. 82–91, May 2018.

[21] P. Regulski, D. S. Vilchis-Rodriguez, S. Djurovic, and V. Terzija, "Estimation of composite load model parameters using an improved particle swarm optimization method," *IEEE Trans. Power Del.*, vol. 30, no. 2, pp. 553–560, Apr. 2015.

[22] Y. Wang, C. Lu, and X. Zhang, "Applicability comparison of different algorithms for ambient signal based load model parameter identification," *Int. J. Electr. Power Energy Syst.*, vol. 111, pp. 382–389, Oct. 2019.

[23] C. Wang, Z. Wang, J. Wang, and D. Zhao, "Robust time-varying parameter identification for composite load modeling," *IEEE Trans. Smart Grid*, vol. 10, no. 1, pp. 967–979, Jan. 2019.

[24] A. M. Najafabadi and A. T. Alouani, "Real time parameter identification of composite load model," in *Proc. IEEE Power Energy Soc. Gen. Meeting*, Jul. 2013, pp. 1–5.

[25] A. Rouhani and A. Abur, "Real-time dynamic parameter estimation for an exponential dynamic load model," *IEEE Trans. Smart Grid*, vol. 7, no. 3, pp. 1530–1536, May 2016.

[26] A. Keyhani, W. Lu, and G. T. Heydt, "Composite neural network load models for power system stability analysis," in *Proc. IEEE PES Power Syst. Conf. Expo.*, Oct. 2004, pp. 1159–1163.

[27] H. R. Kassaei, A. Keyhani, T. Woung, and M. Rahman, "A hybrid fuzzy, neural network bus load modeling and predication," *IEEE Trans. Power Syst.*, vol. 14, no. 2, pp. 718–724, May 1999.

[28] S. Afrasiabi, M. Afrasiabi, B. Parang, and M. Mohammadi, "Integration of accelerated deep neural network into power transformer differential protection," *IEEE Trans. Ind. Informat.*, vol. 16, no. 2, pp. 865–876, Feb. 2020.

[29] J. T. Barron, "A general and adaptive robust loss function," in *Proc. IEEE/CVF Conf. Comput. Vis. Pattern Recognit. (CVPR)*, Jun. 2019, pp. 4331–4339.

[30] D. P. Kingma and J. Ba, "Adam: A method for stochastic optimization," 2014, *arXiv:1412.6980*.

[31] S. Afrasiabi, M. Afrasiabi, B. Parang, and M. Mohammadi, "Designing a composite deep learning based differential protection scheme of power transformers," *Appl. Soft Comput.*, vol. 87, Feb. 2020, Art. no. 105975.

[32] S. Afrasiabi, M. Afrasiabi, M. Mohammadi, and B. Parang, "Fault localisation and diagnosis in transmission networks based on robust deep Gabor convolutional neural network and PMU measurements," *IET Gener., Transmiss. Distrib.*, vol. 14, no. 26, pp. 6484–6492, Dec. 2020.

[33] S. Afrasiabi, M. Mohammadi, M. Afrasiabi, and B. Parang, "Modulated Gabor filter based deep convolutional network for electrical motor bearing fault classification and diagnosis," *IET Sci., Meas. Technol.*, vol. 15, no. 2, pp. 154–162, Mar. 2021.

[34] M. Afrasiabi, M. Mohammadi, M. Rastegar, and S. Afrasiabi, "Advanced deep learning approach for probabilistic wind speed forecasting," *IEEE Trans. Ind. Informat.*, vol. 17, no. 1, pp. 720–727, Jan. 2021.

[35] S. M. H. Rizvi, "Time series deep learning for robust steady-state load parameter estimation using 1D-CNN," *Arabian J. Sci. Eng.*, pp. 1–14, Jun. 2021, doi: 10.1007/s13369-021-05782-6.

[36] M. Afrasiabi, M. Mohammadi, M. Rastegar, and S. Afrasiabi, "Deep learning architecture for direct probability density prediction of small-scale solar generation," *IET Gener., Transmiss. Distrib.*, vol. 14, no. 11, pp. 2017–2025, 2020.

[37] J. H. Chow and K. W. Cheung, "A toolbox for power system dynamics and control engineering education and research," *IEEE Trans. Power Syst.*, vol. 7, no. 4, pp. 1559–1564, Nov. 1992.

[38] M. Amini, A. Jalilian, and M. R. P. Behbahani, "A new method for evaluation of harmonic distortion in reconfiguration of distribution network," *Int. Trans. Electr. Energy Syst.*, vol. 30, no. 6, Jun. 2020, Art. no. e12370.